Applied Mathematics and Computation 393 (2021) 125750

Contents lists available at ScienceDirect

Applied Mathematics and Computation

journal homepage: www.elsevier.com/locate/amc

A class of structure-preserving discontinuous Galerkin variational time integrators for Birkhoffian systems

Chunqiu Wei[a,c], Lin He[b], Huibin Wu[c], Hairui Wen[c,*]

[a] School of Mathematics, Beijing University of Civil Engineering and Architecture, Beijing 102616, China
[b] CSSC Systems Engineering Research Institute, Beijing 100094, China
[c] School of Mathematics and Statistics, Beijing Institute of Technology, Beijing 100081, China

ARTICLE INFO

Article history:
Received 20 April 2020
Revised 24 September 2020
Accepted 15 October 2020
Available online 3 November 2020

Keywords:
Symplectic methods
Variational integrators
Discontinuous Galerkin
Birkhoffian systems

ABSTRACT

Accurate time integrators that preserving Birkhoffian structure are of great practical use for Birkhoffian systems. In this paper, a class of structure-preserving discontinuous Galerkin variational integrators (DGVIs) is presented. Start from the Pfaff action functional, the technique of variational integrators combined with discontinuous Galerkin time discretization is used to derive numerical schemes for Birkhoffian systems. For the derived DGVIs, symplecticity is proved rigorously through the preserving of particular 2-forms induced by these integrators. Linear stability and order of accuracy of the DGVIs are illustrated considering the example of linear damped oscillators. The order of accuracy and the property of preserving conserved quantities of the developed DGVIs are also confirmed by numerical examples. Comparisons are made with several numerical schemes such as backward/forward Euler, Runge–Kutta and RBF methods to show the advantages of DGVIs in preserving the Birkhoffians.

1. Introduction

In [1], Santilli studied the Birkhoffian system in the form

$$\sum_{i=1}^{2n}\left[\frac{\partial R_i(t,\boldsymbol{a})}{\partial a_j}-\frac{\partial R_j(t,\boldsymbol{a})}{\partial a_i}\right]\dot{a}_i-\left[\frac{\partial B(t,\boldsymbol{a})}{\partial a_j}+\frac{\partial R_j(t,\boldsymbol{a})}{\partial t}\right]=0,\quad j=1,2,\ldots,2n, \tag{1.1}$$

where $a_i, R_i(i=1,2,\ldots,2n)$denote the local coordinate, the Birkhoffian function, respectively, and $B$is the Birkhoffian.

The Birkhoffian system (1.1) has a general symplectic structure in geometry, which can describe more general mechanical systems than the Hamiltonian systems, in the sense that the Hamiltonian principle and the Hamiltonian equations are special cases of related Pfaff–Birkhoff principle and Birkhoffian equations [2], respectively. For instance, on the premise without modifying original coordinate variables, the Hojman–Urrutia equation [3] and the Whittaker equation [4], which do not have Hamiltonian representations, can be incorporated into the framework of Birkhoffian systems.

There are quite a few works considering the solvers of ordinary differential equations, such as explicit/implicit Euler methods, the multi-stage Runge–Kutta methods [5], the radial basis function (RBF) collection methods [6], the discontinuous Galerkin (DG) methods [7,8]. For various time-stepping schemes of initial value problems for nonlinear differential

* Corresponding author.
E-mail address: wenhr@bit.edu.cn (H. Wen).

https://doi.org/10.1016/j.amc.2020.125750
0096-3003/

equations, a unified framework was given in [9]. However, the geometrical structure and conserved quantities of system (1.1) are usually difficult to preserve through this approach.

Symplectic methods have the capability of preserving quadratic invariants, which have attracted attentions of many authors. For Hamiltonian problems conserving the Hamiltonian and quadratic invariants, L.Brugnano et al. derived a class of EQUIP integrators [10–13], which is a symplectic variant of the s-stage Gauss collocation methods with energy-preserving properties. And also symplectic variational integrators are designed by others regarding different dynamical systems, for instance, for Lagrangian systems [14], Hamiltonian systems [15], Birkhoffian systems [16,17], nonholonomic systems [18], non-smooth collisions [19], optimal control [20], and constrained systems [21]. A survey of the symplectic variational integrators in discrete mechanics can be found in [22].

For the Birkhoffian system (1.1), it is a challenge to design numerical methods to retain geometric properties and conserved quantities. The related variational structure provides an ideal framework, in this treatment, the so-called variational integrators usually exhibit excellent structure-preserving properties such as symplecticity, momentum and energy preserving. Variational integrators is based on first finding the variational form of system (1.1), and then approximating the variational form by finite differences, finite element methods or spectral methods. Since the variational integrator techniques inherit the variational structure of the mechanical systems, the geometric properties of the differential system are usually retained automatically.

The discontinuous Galerkin (DG) discretization combined with the variational integrators was first introduced by Gagarina et al. in [23,24] for Hamiltonian systems. As a local polynomial is used in each time subinterval, the numerical flux, which connects the solutions of adjacent subintervals, is the heart of the DG discretizations. In [23,24], the authors verified the symplecticity of different numerical schemes, numerical results therein also reflect excellent quantity preserving properties for Hamiltonian systems. For the Birkhoffian systems (1.1), it does make sense to construct high order, stable numerical integrators that preserve the symplectic structure and particular conserved quantities at discrete level, and variational integrators combined with DG techniques provides an optional attempt.

Unlike the integrators proposed in [16], which used finite differences to approximate the time derivatives in the Pfaff action functional, we use discontinuous Galerkin techniques and adopt a similar numerical flux given in [23,24] to discretize the Pfaff action functional. The main works of this paper are summarized as follows.

1. Combining variational formulation with discontinuous Galerkin time discretization, we derive a class of stable, structure-preserving DGVIs, which can be generalized to arbitrary high order. Schemes proposed in [16] are shown to be special cases of our lower-order DGVIs, and we also propose a novel third-order integrators for Birkhoffian system (1.1).
2. For the derived DGVIs, symplecticity have been proved rigorously. Linear stability of the DGVIs is illustrated considering the example of linear damped oscillators, error estimates are also given for the first-order and second-order DGVIs. The order of accuracy and preservation of Birkhoffians are numerically confirmed for all the three DGVIs in the last section.

This paper is organized as follows. In Section 2, we introduce the symplectic structure of the Birkhoffian systems (1.1). In Section 3.1, we give the procedure to design DGVIs, and in Sections 3.2–3.3, we propose a class of DGVIs from the first-order to the third-order in the sequel. In Section 4, we prove the symplecticity and present linear stability, error estimates of the above mentioned DGVIs. To validate the proposed DGVIs, numerical tests are presented in Section 5, where advantages of DGVIs in preserving Birkhoffians are also showed through the comparisons between DGVIs and other numerical schemes. Conclusions are given in Section 6.

2. Symplectic structure of the Birkhoffian systems (1.1)

Let Mbe a $2n$-dimension manifold with local coordinates $\boldsymbol{a} = (a_1, a_2, \ldots, a_{2n})$,for time interval $[t_0, t_f]$,denote the path space from $\boldsymbol{a}_0 = \boldsymbol{a}(t_0)$to $\boldsymbol{a}_f = \boldsymbol{a}(t_f)$by

$$P(\boldsymbol{a}_0, \boldsymbol{a}_f, [t_0, t_f]) = \{\boldsymbol{a} : [t_0, t_f] \to M |\ \boldsymbol{a} \in C^2([t_0, t_f])\}.$$

The Pfaff action functional $\mathcal{A}(\boldsymbol{a}) : P(\boldsymbol{a}_0, \boldsymbol{a}_f, [t_0, t_f]) \to \mathbb{R}$is given by

$$\mathcal{A}(\boldsymbol{a}) = \int_{t_0}^{t_f} \left[\sum_{i=1}^{2n} R_i(t, \boldsymbol{a}) \dot{a}_i(t) - B(t, \boldsymbol{a}) \right] \mathrm{d}t. \tag{2.1}$$

Derivation of the Birkhoffian systems (1.1) from the Pfaff action functional (2.1) can be found in [16, Section 2], we omit the detail here. Now we give the structure matrix $G(t, \boldsymbol{a})$of the Birkhoffian system (1.1)

$$G(t, \boldsymbol{a}) = (G_{ij})_{2n\times 2n} = \left(\frac{\partial R_j}{\partial a_i} - \frac{\partial R_i}{\partial a_j} \right)_{2n\times 2n}, \quad \text{for} \quad i, j = 1, 2, \ldots, 2n. \tag{2.2}$$

Then, from the geometrical point of view, the Birkhoffian system (1.1) possess a natural symplectic structure, which is given by the following Birkhoffian symplectic form

$$\Omega_B = \frac{1}{2}\sum_{i=1}^{2n}\sum_{j=1}^{2n} G_{ji}\mathrm{d}a_j \wedge \mathrm{d}a_i. \tag{2.3}$$

Remark 2.1. Let $B = H, R_i = 0, R_{n+i} = a_i (i = 1, \ldots, n)$in the Birkhoff system (1.1), one can obtain the classical Hamiltonian system (for simplicity, we use $n = 1$.)

$$\begin{cases} \frac{da_2}{dt} - \frac{\partial H}{\partial a_1} = 0, \\ \frac{da_1}{dt} + \frac{\partial H}{\partial a_2} = 0. \end{cases}$$

In the meanwhile, the Birkhoffian symplectic form (2.3) will reduce to the canonical symplectic form $\sum_{i=1}^{n} \mathrm{d}a_i \wedge \mathrm{d}a_{n+i}$.

3. Discretization of the Birkhoffian system (1.1)

In this section, based on the Pfaff action functional (2.1), we derive a class of DGVIs for the Birkhoffian system (1.1).

3.1. Discrete Pfaff action functional

First we divide the time interval $[t_0, t_f]$to form a uniform grid with grid points $\{t_k\}, k = 0, 1, \ldots, K$,where $t_K = t_f$,and denote by $I_k = (t_{k-1}, t_k)$and mesh size $\tau = t_k - t_{k-1}$. Here the uniform grids are taken for easy presentation, nonuniform grids work as well. In each time subinterval I_k,the numerical approximation is a polynomial $a_i^\tau|_{I_k} = a_i^{\tau,k} \in P^s, i = 1, 2, \ldots, 2n$,where P^sdenotes the linear space of all polynomials of degree at most s:

$$P^s := \{p \mid p(x)|_{I_k} = \sum_{j=0}^{s} q_j (x - x_k)^j,\ q_j \in \mathbb{R},\ s \in \mathbb{N}^+\}. \tag{3.1}$$

Let $v(x^\pm) = \lim_{\epsilon\to 0\pm} v(x+\epsilon)$and $v_k^\pm = v(x_k^\pm)$. The jump and average at $t_k$are

$$[v]|_{t_k} = v^{k,+} - v^{k,-},\ \ \{v\}|_{t_k,\alpha} = \alpha v^{k,+} + (1-\alpha)v^{k,-}, \tag{3.2}$$

respectively, for $\alpha \in [0, 1]$.

By introducing the solution representative a_i^τinto the action functional (2.1) and splitting the time integral into a summation over time intervals I_k,we obtain the discrete action functional

$$\mathcal{A}^\tau(\boldsymbol{a}^\tau) = \sum_{k=1}^{K}\int_{t_{k-1}}^{t_k}\left[\sum_{i=1}^{2n} R_i(t, \boldsymbol{a}^\tau)\dot{a}_i^\tau(t) - B(t, \boldsymbol{a}^\tau)\right]\mathrm{d}t + \sum_{k=1}^{K}\sum_{i=1}^{2n}[a_i^\tau]\{R_i(t, \boldsymbol{a}^\tau)\}|_{t_k,\alpha}. \tag{3.3}$$

Since we use discontinuous basis functions, the last term of (3.3) plays the role of numerical flux (for derivations of this type of numerical flux, cf. [23, Appendix C] [24]). Then, to approximate the integrals in (3.3), we select a suitable quadrature rule which is corresponding to the degree of polynomial solution representative and the attainable order of DGVIs. As is proven in [25], the order of the quadrature rule will give an upper bound for the order of the variational integrators.

The strategy of our numerical schemes (DGVIs) is listed as follows:

1. Specify the degree $s$of the polynomial solution representative a_i^τ,which is discontinuous at each grid point t_k;
2. In subinterval I_k,set $a_i^\tau = \sum_j q_j\phi_j$,where $\{\phi_j\}$denote some basis functions, for instance, Lagrange basis functions, and $q_j$is the coordinate of a_i^τaccording to ϕ_j;
3. Select an appropriate quadrature rule of order $s+1$to calculate the time integrals in (3.3), and the discrete functional $\mathcal{A}^\tau(\boldsymbol{a}^\tau)$now can be taken as a function of the independent variables $\{q_j\}$;
4. Taking variation of the discrete functional $\mathcal{A}^\tau(\boldsymbol{a}^\tau)$and collecting the common terms with respect to δq_j,a linear (or nonlinear) algebraic system in unknowns $\{q_j\}$is obtained, which formulate our numerical schemes (DGVIs).

3.2. Rederivation of a first-order scheme

In this section, following the strategy outlined at the end of Section 3.1, we propose a first-order numerical scheme **P0L1O1** for the Birkhoffian system (1.1). We would like to comment that the first-order scheme given in [16] is a special case of the first-order DGVIs, cf. Remark 3.1.

Case 1(P0L1O1): Choose piecewise constant function a_i^k(P0) as the solution representative in time interval I_k,and use the left rectangle rule (L1) to approximate the exact integrals in action functional (3.3), then the DGVIs is of first-order (O1). As terms containing derivatives vanish, the discrete action functional (3.3) can be written as

$$\mathcal{A}^\tau(\boldsymbol{a}^\tau) = \sum_{k=1}^{K}\sum_{i=1}^{2n}(a_i^k - a_i^{k-1})\left(\alpha R_i^k + (1-\alpha)R_i^{k-1}\right) - \tau\sum_{k=1}^{K} B^{k-1}, \tag{3.4}$$

where $R_i^k = R_i(t_k, \boldsymbol{a}^k)$, $B^{k-1} = B(t_{k-1}, \boldsymbol{a}^{k-1})$.

Taking variation of $\mathcal{A}^\tau(\boldsymbol{a}^\tau)$in (3.4), we obtain

$$\begin{aligned}\delta\mathcal{A}^\tau(\boldsymbol{a}^\tau) = &\sum_{k=1}^{K}\sum_{i=1}^{2n}(\delta a_i^k - \delta a_i^{k-1})\left[\alpha R_i^k + (1-\alpha)R_i^{k-1}\right]\\ &+\sum_{k=1}^{K}\sum_{i=1}^{2n}(a_i^k - a_i^{k-1})\left[\alpha\sum_{j=1}^{2n}\frac{\partial R_i^k}{\partial a_j^k}\delta a_j^k + (1-\alpha)\sum_{j=1}^{2n}\frac{\partial R_i^{k-1}}{\partial a_j^{k-1}}\delta a_j^{k-1}\right] - \tau\sum_{k=1}^{K}\sum_{j=1}^{2n}\frac{\partial B^{k-1}}{\partial a_j^{k-1}}\delta a_j^{k-1}.\end{aligned} \tag{3.5}$$

Setting $\delta a_j^{-1} = \delta a_j^K = 0$,collecting the common terms containing δa_j^k,by the variational principle $\delta\mathcal{A}^\tau(\boldsymbol{a}^\tau) = 0$and the arbitrariness of δa_j^k,scheme **P0L1O1** is given by

$$\sum_{i=1}^{2n}\left[(1-\alpha)a_i^k - (1-2\alpha)a_i^{k-1} - \alpha a_i^{k-2}\right]\frac{\partial R_i^{k-1}}{\partial a_j^{k-1}} - \left[\alpha R_j^k + (1-2\alpha)R_j^{k-1} - (1-\alpha)R_j^{k-2}\right] - \tau\frac{\partial B^{k-1}}{\partial a_j^{k-1}} = 0. \tag{3.6}$$

Remark 3.1. (1) If we set $\alpha = 0$and use the right rectangle rule to approximate the integrals in the discrete action functional (3.3), or equivalently, take $\alpha = 0$and $k = k+1$in (3.4), the first-order approximation (10) in [16] can be recovered. Then the first-order Kong's method is the same as "P0R1O1" in DGVIs, with "R1" standing for the first-order right rectangle quadrature rule.

(2) If take $t_{k-\frac{1}{2}} = (t_k + t_{k-1})/2, \boldsymbol{a}^{k-\frac{1}{2}} = (\boldsymbol{a}^k + \boldsymbol{a}^{k-1})/2$,then replace the average term $\{R_i(t, \boldsymbol{a}^\tau)\}|_{t_k,\alpha}$and $B(t, a^\tau)$in functional (3.3) by $R_i^{k-\frac{1}{2}} = R_i(t_{k-\frac{1}{2}}, \boldsymbol{a}^{k-\frac{1}{2}})$and $B^{k-\frac{1}{2}} = B(t_{k-\frac{1}{2}}, \boldsymbol{a}^{k-\frac{1}{2}})$,respectively, the second-order Kong's method (21) in [16] can be recovered.

3.3. High-order DGVIs for Birkhoffian system (1.1)

In this section, with piecewise linear and piecewise quadratic polynomials as the solution representative, then choosing appropriate numerical quadrature rule to approximate the time integrals in the action functional (3.3), we derive the following two DGVIs for Birkhoffian system (1.1).

Case 2(P1M2O2): Using linear function $a_i^{\tau,k}$(P1) in (3.7) as the solution representative in interval I_k,then choosing the midpoint rule (M2) to approximate the exact integrals in (3.3) so that the order (O2) of the function approximating step agree with that of the integration step, we obtain the second-order DGVI (3.10).

Noting that the solution representative $a_i^{\tau,k}$is linear in t

$$a_i^{\tau,k} = \frac{t_k - t}{\tau}a_i^{k-1,+} + \frac{t - t_{k-1}}{\tau}a_i^{k,-}, \tag{3.7}$$

in which $a_i^{\cdot,\pm}$are unknowns to be determined, substituting (3.7) into the integral terms of (3.3) and applying the midpoint rule gives

$$\int_{t_{k-1}}^{t_k}\sum_{i=1}^{2n}R_i(t, \boldsymbol{a}^\tau)\dot{a}_i^{\tau,k}\,\mathrm{d}t = \sum_{i=1}^{2n}R_i^{k-\frac{1}{2}}(a_i^{k,-} - a_i^{k-1,+}) \tag{3.8}$$

and

$$\int_{t_{k-1}}^{t_k}B(t, \boldsymbol{a}^\tau)\,\mathrm{d}t = \tau B^{k-\frac{1}{2}}, \tag{3.9}$$

where $\boldsymbol{a}^{k-\frac{1}{2}}$can be calculated from (3.7) for $t = (t_{k-1} + t_k)/2, R_i^{k-\frac{1}{2}} = R_i(t_{k-\frac{1}{2}}, \boldsymbol{a}^{k-\frac{1}{2}}), B^{k-\frac{1}{2}} = B(t_{k-\frac{1}{2}}, \boldsymbol{a}^{k-\frac{1}{2}})$.

Substituting (3.8), (3.9) into (3.3) and using (3.7), we have

$$\mathcal{A}^\tau(\boldsymbol{a}^\tau) = \sum_{k=1}^{K}\left[\sum_{i=1}^{2n}R_i^{k-\frac{1}{2}}(a_i^{k,-} - a_i^{k-1,+}) - \tau B^{k-\frac{1}{2}}\right] + \sum_{k=0}^{K}\sum_{i=1}^{2n}(a_i^{k,+} - a_i^{k,-})\left[\alpha R_i^{k,+} + (1-\alpha)R_i^{k,-}\right].$$

Similar to **Case 1**, taking variation of $\mathcal{A}^\tau(\boldsymbol{a}^\tau)$with respect to $a_j^{k-1,+}$, $a_j^{k,-}$,then by the variational principle $\delta\mathcal{A}^\tau(\boldsymbol{a}^\tau) = 0$and endpoint conditions $\delta a_j^{0,-} = \delta a_j^{K,+} = 0$,we obtain the following scheme **P1M2O2**,

$$\begin{cases}\sum_{i=1}^{2n}\left(\frac{1}{2}(a_i^{k,-} - a_i^{k-1,+})\frac{\partial R_i^{k-\frac{1}{2}}}{\partial a_j^{k-\frac{1}{2}}} + \alpha(a_i^{k-1,+} - a_i^{k-1,-})\frac{\partial R_i^{k-1,+}}{\partial a_j^{k-1,+}}\right) - R_j^{k-\frac{1}{2}}\\ -\frac{1}{2}\tau\frac{\partial B^{k-\frac{1}{2}}}{\partial a_j^{k-\frac{1}{2}}} + \left(\alpha R_j^{k-1,+} + (1-\alpha)R_j^{k-1,-}\right) = 0,\\ \sum_{i=1}^{2n}\left(\frac{1}{2}(a_i^{k,-} - a_i^{k-1,+})\frac{\partial R_i^{k-\frac{1}{2}}}{\partial a_j^{k-\frac{1}{2}}} + (1-\alpha)(a_i^{k,+} - a_i^{k,-})\frac{\partial R_i^{k,-}}{\partial a_j^{k,-}}\right) + R_j^{k-\frac{1}{2}}\\ -\frac{1}{2}\tau\frac{\partial B^{k-\frac{1}{2}}}{\partial a_j^{k-\frac{1}{2}}} - \left(\alpha R_j^{k,+} + (1-\alpha)R_j^{k,-}\right) = 0.\end{cases} \tag{3.10}$$

Case 3(P2S3O3): Using the following quadratic polynomial $a_i^{\tau,k}$(P2) as the solution representative, choosing the Simpson's rule (S3) to approximate the integrals in (3.3), we obtain the third-order (O3) DGVI (3.11).

In time interval I_k,using quadratic Lagrange basis functions, the numerical solution $a_i^{\tau,k}$is given by

$$a_i^{\tau,k}=\frac{(t_{k-1}+t_k-2t)(t_k-t)}{\tau^2}a_i^{k-1,+}+4\frac{(t-t_{k-1})(t_k-t)}{\tau^2}a_i^{k-\frac{1}{2}}-\frac{(t_{k-1}+t_k-2t)(t-t_{k-1})}{\tau^2}a_i^{k,-},$$

in which $a_i^{\cdot,\pm}$and $a_i^{k-\frac{1}{2}}$are unknowns to be determined. Similar to **Case 1** and **Case 2**, now the discrete action functional becomes

$$\begin{aligned}\mathcal{A}^\tau(\boldsymbol{a}^\tau)=&\frac{1}{6}\sum_{k=1}^{K}\sum_{i=1}^{2n}\Big[(-3a_i^{k-1,+}+4a_i^{k-\frac{1}{2}}-a_i^{k,-})R_i^{k-1,+}+4(a_i^{k,-}-a_i^{k-1,+})R_i^{k-\frac{1}{2}}\\&+(a_i^{k-1,+}-4a_i^{k-\frac{1}{2}}+3a_i^{k,-})R_i^{k,-}\Big]-\frac{\tau}{6}\sum_{k=1}^{K}(B^{k-1,+}+4B^{k-\frac{1}{2}}+B^{k,-})\\&+\sum_{k=0}^{K}\sum_{i=1}^{2n}(a_i^{k,+}-a_i^{k,-})\big[\alpha R_i^{k,+}+(1-\alpha)R_i^{k,-}\big].\end{aligned}$$

And the third-order DGVI (**P2S3O3**) is

$$\begin{cases}\sum_{i=1}^{2n}\Big[-3a_i^{k-1,+}+4a_i^{k-\frac{1}{2}}-a_i^{k,-}+6\alpha(a_i^{k-1,+}-a_i^{k-1,-})\Big]\frac{\partial R_i^{k-1,+}}{\partial a_j^{k-1,+}}\\\quad-3R_j^{k-1,+}-4R_j^{k-\frac{1}{2}}+R_j^{k,-}+6\big(\alpha R_j^{k-1,+}+(1-\alpha)R_j^{k-1,-}\big)-\tau\frac{\partial B^{k-1,+}}{\partial a_j^{k-1,+}}=0,\\\sum_{i=1}^{2n}(a_i^{k,-}-a_i^{k-1,+})\frac{\partial R_i^{k-\frac{1}{2}}}{\partial a_j^{k-\frac{1}{2}}}+R_j^{k-1,+}-R_j^{k,-}-\tau\frac{\partial B^{k-\frac{1}{2}}}{\partial a_j^{k-\frac{1}{2}}}=0,\\\sum_{i=1}^{2n}\Big[a_i^{k-1,+}-4a_i^{k-\frac{1}{2}}+3a_i^{k,-}+6(1-\alpha)(a_i^{k,+}-a_i^{k,-})\Big]\frac{\partial R_i^{k,-}}{\partial a_j^{k,-}}\\\quad-R_j^{k-1,+}+4R_j^{k-\frac{1}{2}}+3R_j^{k,-}-6\big(\alpha R_j^{k,+}+(1-\alpha)R_j^{k,-}\big)-\tau\frac{\partial B^{k,-}}{\partial a_j^{k,-}}=0.\end{cases}\tag{3.11}$$

In Section 4, the above three schemes **P0L1O1, P1M2O2** and **P2S3O3** are proven to be symplectic. Numerical experiments in Section 5 show that these schemes exhibit excellent approximations to both the exact solution and the conserved quantity Birkhoffian.

4. Properties of the DGVIs for Birkhoffian system (1.1)

As we know, numerical schemes define flow maps that transfer given initial data to corresponding final states. The symplecticity of a numerical scheme means: the sum of the oriented areas of the projections of a parallelogram onto the state space is conserved by the flow map [26]. For the first-order scheme **P0L1O1** when $\alpha=0$,symplecticity has been proved in [16] by showing that the related flow map preserves an induced 2-form [22].

In this section, for schemes **P0L1O1, P1M2O2** and **P2S3O3** proposed in Section 3, we prove the symplecticity in Section 4.1 and linear stability is illustrated in Section 4.2 on the linear damped oscillator example.

4.1. Symplecticity

Recall the definition of $G(t,\boldsymbol{a})$-symplectic [27]of a differentiable mapping.

Definition 4.1. [$G(t,\boldsymbol{a})$-symplectic] A differentiable mapping $g:[t_0,t_f]\times M\to M$is $G(t,\boldsymbol{a})$-symplectic if the Jacobian $\frac{\partial g}{\partial \boldsymbol{a}}$satisfies

$$\left(\frac{\partial g}{\partial \boldsymbol{a}}\right)^T G(t,g(t,\boldsymbol{a}))\left(\frac{\partial g}{\partial \boldsymbol{a}}\right)=G(t_0,\boldsymbol{a}),\tag{4.1}$$

where $G(t,\boldsymbol{a})$denotes the structure matrix (2.2). And an explicit scheme $\boldsymbol{a}^k=g^{k-1}(t_{k-1},\boldsymbol{a}^{k-1})$approximating the Birkhoffian system (1.1) is $G(t,\boldsymbol{a})$-symplectic if

$$\left(\frac{\partial g^{k-1}}{\partial \boldsymbol{a}^{k-1}}\right)^T G(t_k,\boldsymbol{a}^k)\left(\frac{\partial g^{k-1}}{\partial \boldsymbol{a}^{k-1}}\right)=G(t_{k-1},\boldsymbol{a}^{k-1}).\tag{4.2}$$

For general Birkhoffian function $R_i(t,\boldsymbol{a})$and Birkhoffian $B(t,\boldsymbol{a})$,if using Definition 4.1, the Jacobian matrix of $g^{k-1}(t_{k-1},\boldsymbol{a}^{k-1})$related to DGVIs is usually too complex to present explicitly, so we choose to prove that the flow map induced by $g^{k-1}(t_{k-1},\boldsymbol{a}^{k-1})$preserves the related 2-form, which is equivalent to Definition 4.1 ([26, Chapter VI, Lemma 2.3]),

as what we will do in Theorem 4.1. But for given concrete examples, using Definition 4.1, the symplecticity of a numerical scheme can be verified in a much easier way, we only need to show that the mapping $g^{k-1}(t_{k-1}, \boldsymbol{a}^{k-1})$(or expanded mapping for multi-level schemes) satisfies (4.2), as what we do in Section 5.

Theorem 4.1. *For the Birkhoffian system (1.1), schemes* ***P0L1O1*** *(3.6),* ***P1M2O2*** *(3.10) and* ***P2S3O3*** *(3.11) are all symplectic.*

Proof. To prove the symplecticity of scheme **P0L1O1** (3.6) for general α,calculating the derivative of (3.4) and collecting common terms give

$$\begin{aligned}
\mathrm{d}\mathcal{A}^{\tau}(\boldsymbol{a}^{\tau})\cdot\delta\boldsymbol{a}^{\tau} =& \sum_{k=1}^{K}\sum_{j=1}^{2n}\Bigg[\sum_{i=1}^{2n}\Big((1-\alpha)a_i^k-(1-2\alpha)a_i^{k-1}-\alpha a_i^{k-2}\Big)\frac{\partial R_i^{k-1}}{\partial a_j^{k-1}}\\
&-\Big[\alpha R_j^k+(1-2\alpha)R_j^{k-1}-(1-\alpha)R_j^{k-2}\Big]-\tau\frac{\partial B^{k-1}}{\partial a_j^{k-1}}\Bigg]\delta a_j^{k-1}\\
&+\sum_{j=1}^{2n}\Bigg[\sum_{i=1}^{2n}\alpha(a_i^K-a_i^{K-1})\frac{\partial R_i^K}{\partial a_j^K}+\Big(\alpha R_j^K+(1-\alpha)R_j^{K-1}\Big)\Bigg]\delta a_j^K\\
&+\sum_{j=1}^{2n}\Bigg[\sum_{i=1}^{2n}(1-\alpha)(a_i^0-a_i^{-1})\frac{\partial R_i^{-1}}{\partial a_j^{-1}}-\Big(\alpha R_j^0+(1-\alpha)R_j^{-1}\Big)\Bigg]\delta a_j^{-1}\\
=&\Theta^{+}(\boldsymbol{a}^{K-1},\boldsymbol{a}^{K})\cdot(\delta a_j^{K-1},\delta a_j^{K})-\Theta^{-}(\boldsymbol{a}^{-1},\boldsymbol{a}^{0})\cdot(\delta a_j^{-1},\delta a_j^{0}),
\end{aligned}\tag{4.3}$$

where in the last equality we have used (3.6), 1-forms (cf. [22, Theorem 1.3.1])

$$\Theta^{+}(\boldsymbol{a}^{k-1},\boldsymbol{a}^{k})=\sum_{j=1}^{2n}\Bigg[\sum_{i=1}^{2n}\alpha(a_i^k-a_i^{k-1})\frac{\partial R_i^k}{\partial a_j^{k-1}}+\Big(\alpha R_j^k+(1-\alpha)R_j^{k-1}\Big)\Bigg]\mathrm{d}a_j^k\tag{4.4}$$

and

$$\Theta^{-}(\boldsymbol{a}^{k-1},\boldsymbol{a}^{k})=-\sum_{j=1}^{2n}\Bigg[\sum_{i=1}^{2n}(1-\alpha)(a_i^k-a_i^{k-1})\frac{\partial R_i^{k-1}}{\partial a_j^{k-1}}-\Big(\alpha R_j^k+(1-\alpha)R_j^{k-1}\Big)\Bigg]\mathrm{d}a_j^{k-1}.\tag{4.5}$$

Taking differential of (4.4) and (4.5), we obtain

$$\mathrm{d}\Theta^{+}(\boldsymbol{a}^{k-1},\boldsymbol{a}^{k})=\sum_{j=1}^{2n}\sum_{i=1}^{2n}\Bigg[-\alpha\frac{\partial R_i^k}{\partial a_j^k}+(1-\alpha)\frac{\partial R_j^{k-1}}{\partial a_i^{k-1}}\Bigg]\mathrm{d}a_i^{k-1}\wedge\mathrm{d}a_j^k,\tag{4.6}$$

$$\mathrm{d}\Theta^{-}(\boldsymbol{a}^{k-1},\boldsymbol{a}^{k})=-\sum_{j=1}^{2n}\sum_{i=1}^{2n}\Bigg[(1-\alpha)\frac{\partial R_i^{k-1}}{\partial a_j^{k-1}}-\alpha\frac{\partial R_j^k}{\partial a_i^k}\Bigg]\mathrm{d}a_i^{k}\wedge\mathrm{d}a_j^{k-1}.\tag{4.7}$$

Then, rearrangement of the summation and the anticommutative property of cross product lead to

$$\mathrm{d}\Theta^{+}(\boldsymbol{a}^{k-1},\boldsymbol{a}^{k})=\mathrm{d}\Theta^{-}(\boldsymbol{a}^{k-1},\boldsymbol{a}^{k}).\tag{4.8}$$

Hence, we can define a single 2-form $\Omega(\cdot,\cdot)$as

$$\Omega(\boldsymbol{a}^{k-1},\boldsymbol{a}^{k})=\mathrm{d}\Theta^{+}(\boldsymbol{a}^{k-1},\boldsymbol{a}^{k}).\tag{4.9}$$

Furthermore, from (3.6), we define an expanded flow map $G(\cdot,\cdot)$as

$$(\boldsymbol{a}^{k},\boldsymbol{a}^{k+1})=G(\boldsymbol{a}^{k-1},\boldsymbol{a}^{k}),$$

in which the initial condition is $(\boldsymbol{a}^{-1},\boldsymbol{a}^{0})=(\boldsymbol{a}^{0},\boldsymbol{a}^{0})$,the action functional $\mathcal{A}^{\tau}(\boldsymbol{a}^{\tau})$can thus be restricted as

$$\hat{\mathcal{A}}(\boldsymbol{a}^{-1},\boldsymbol{a}^{0})=\mathcal{A}^{\tau}(\boldsymbol{a}^{\tau}),\tag{4.10}$$

with $\hat{\mathcal{A}}: M\times M\to\mathbb{R}$. Calculating the derivative of the restricted action functional $\hat{\mathcal{A}}(\boldsymbol{a}^{-1},\boldsymbol{a}^{0})$gives

$$\begin{aligned}
\mathrm{d}\hat{\mathcal{A}}(\boldsymbol{a}^{-1},\boldsymbol{a}^{0})\cdot(\delta\boldsymbol{a}^{-1},\delta\boldsymbol{a}^{0}) =&\mathrm{d}\mathcal{A}^{\tau}(\boldsymbol{a}^{\tau})\cdot\delta\boldsymbol{a}^{\tau}\\
=&\Theta^{+}(\boldsymbol{a}^{K-1},\boldsymbol{a}^{K})\cdot(\delta\boldsymbol{a}^{K-1},\delta\boldsymbol{a}^{K})-\Theta^{-}(\boldsymbol{a}^{-1},\boldsymbol{a}^{0})\cdot(\delta\boldsymbol{a}^{-1},\delta\boldsymbol{a}^{0})\\
=&\Theta^{+}\Big(G^{K}(\boldsymbol{a}^{-1},\boldsymbol{a}^{0})\Big)\cdot\Big(\big(G^{K}\big)_{*}(\delta\boldsymbol{a}^{-1},\delta\boldsymbol{a}^{0})\Big)-\Theta^{-}(\boldsymbol{a}^{-1},\boldsymbol{a}^{0})\cdot(\delta\boldsymbol{a}^{-1},\delta\boldsymbol{a}^{0})\\
=&\Big(\big(G^{K}\big)^{*}\Theta^{+}\Big)(\boldsymbol{a}^{-1},\boldsymbol{a}^{0})\cdot(\delta\boldsymbol{a}^{-1},\delta\boldsymbol{a}^{0})-\Theta^{-}(\boldsymbol{a}^{-1},\boldsymbol{a}^{0})\cdot(\delta\boldsymbol{a}^{-1},\delta\boldsymbol{a}^{0}),\\
=&\Big(\big(G^{K}\big)^{*}\Theta^{+}-\Theta^{-}\Big)(\boldsymbol{a}^{-1},\boldsymbol{a}^{0})\cdot(\delta\boldsymbol{a}^{-1},\delta\boldsymbol{a}^{0}),
\end{aligned}\tag{4.11}$$

where we have used (4.3) in the second equality,

$$(\boldsymbol{a}^{K-1}, \boldsymbol{a}^{K}) = G^{K}(\boldsymbol{a}^{-1}, \boldsymbol{a}^{0}), \tag{4.12}$$

$$\left(G^{K}\right)_{*}(\delta\boldsymbol{a}^{-1}, \delta\boldsymbol{a}^{0}) = (\delta\boldsymbol{a}^{K-1}, \delta\boldsymbol{a}^{K}) \tag{4.13}$$

in the third equality and

$$\left(\left(G^{K}\right)^{*}\Theta^{+}\right)(\boldsymbol{a}^{-1}, \boldsymbol{a}^{0}) \cdot (\delta\boldsymbol{a}^{-1}, \delta\boldsymbol{a}^{0}) = \Theta^{+}\left(G^{K}(\boldsymbol{a}^{-1}, \boldsymbol{a}^{0})\right) \cdot \left(\left(G^{K}\right)_{*}(\delta\boldsymbol{a}^{-1}, \delta\boldsymbol{a}^{0})\right) \tag{4.14}$$

in the fourth equality of (4.11) (cf. Remark 4.1).

From the last equality of (4.11), we claim that

$$\mathrm{d}\hat{\mathcal{A}} = \left(G^{K}\right)^{*}\Theta^{+} - \Theta^{-}, \tag{4.15}$$

then taking differential of (4.15), noting the fact $\mathrm{d}^2 = 0$,utilizing (4.9) and (4.8), we obtain

$$\left(G^{K}\right)^{*}\Omega = \Omega. \tag{4.16}$$

The above argument leading to (4.16) holds true for any time interval $[t_0, t_k](k = 1, \ldots, K)$,which implies that the flow map Gpreserves the 2-form Ωdefined by (4.9), that is, scheme **P0L1O1** (3.6) is symplectic (see [22, Section 1.3.2]).

Now we turn to the symplecticity of scheme **P1M2O2** (3.10) and **P2S3O3** (3.11), instead of (4.4) and (4.5) for scheme **P0L1O1**, we can define two 1-forms for both schemes as

$$\Theta^{+}(\boldsymbol{a}^{k,-}, \boldsymbol{a}^{k,+}) = \sum_{j=1}^{2n}\left[\sum_{i=1}^{2n}\alpha(a_i^{k,+} - a_i^{k,-})\frac{\partial R_i^{k,+}}{\partial a_j^{k,+}} + \left(\alpha R_j^{k,+} + (1-\alpha)R_j^{k,-}\right)\right]\mathrm{d}a_j^{k,+}, \tag{4.17}$$

$$\Theta^{-}(\boldsymbol{a}^{k,-}, \boldsymbol{a}^{k,+}) = -\sum_{j=1}^{2n}\left[\sum_{i=1}^{2n}(1-\alpha)(a_i^{k,+} - a_i^{k,-})\frac{\partial R_i^{k,-}}{\partial a_j^{k,-}} - \left(\alpha R_j^{k,+} + (1-\alpha)R_j^{k,-}\right)\right]\mathrm{d}a_j^{k,-}. \tag{4.18}$$

Similar to the proof for scheme **P0L1O1**, as $\mathrm{d}\Theta^{+}(\boldsymbol{a}^{k,-}, \boldsymbol{a}^{k,+}) = \mathrm{d}\Theta^{-}(\boldsymbol{a}^{k,-}, \boldsymbol{a}^{k,+})$,define the 2-form by $\Omega(\boldsymbol{a}^{k,-}, \boldsymbol{a}^{k,+}) = \mathrm{d}\Theta^{+}(\boldsymbol{a}^{k,-}, \boldsymbol{a}^{k,+})$,then follow the same argument leading to (4.16), we can prove the expanded flow maps related to schemes **P1M2O2** and **P2S3O3** preserve the corresponding 2-form $\Omega(\cdot,\cdot)$. This completes the proof of Theorem 4.1.

□

Remark 4.1. In [28, Chapter 4], $\left(G^{K}\right)_{*}(\delta\boldsymbol{a}^{-1}, \delta\boldsymbol{a}^{0})$(4.12) is called a push-forward of $(\delta\boldsymbol{a}^{-1}, \delta\boldsymbol{a}^{0})$and $\left(G^{K}\right)^{*}\Theta^{+}$in (4.14) is called a pull-back of 1-form Θ^{+}.

4.2. Linear stability

The root condition is a necessary and sufficient condition for the boundedness (stability) of solutions to linear multistep difference equations [29, Theorem 3.3.14]. To ensure the stability of numerical solutions computed through the DGVIs, it is required that the eigenvalues of the iteration matrix corresponding to the DGVIs are all less than or equal to 1 in modulus, where the latter have to be simple. In this section, linear stability of the DGVIs proposed in Section 3 is verified on the linear damped oscillators which have quadratic Birkhoffians as an example. As we will see, interestingly, the moduli of the eigenvalues do not rely on the parameter α,for **P0L1O1** and **P1M2O2**, the moduli of eigenvalues of the iteration matrix are always $e^{-\gamma\tau/2}$for $\gamma \in [0, 2]$,the eigenvalues of **P2S3O3** are too complex to present explicitly, but the moduli of eigenvalues are still $e^{-\gamma\tau/2}$,which can be numerically verified.

The linear damped oscillators are governed by the following equation

$$\ddot{x} + \gamma\dot{x} + x = 0, \tag{4.19}$$

with $\gamma \in [0, 2]$being a positive constant.

Let $a_1 = x, a_2 = \dot{x}$in (1.1), (4.19) has a Birkhoffian representation

$$\begin{cases} R_1(t, \mathbf{a}) = \frac{1}{2}e^{\gamma t}a_2, \ R_2(t, \mathbf{a}) = -\frac{1}{2}e^{\gamma t}a_1, \\ B(t, \mathbf{a}) = \frac{1}{2}e^{\gamma t}\left[(a_1)^2 + (a_2)^2 + \gamma a_1 a_2\right]. \end{cases} \tag{4.20}$$

Case 1(P0L1O1): Substitute (4.20) into scheme **P0L1O1** (3.6) and write the scheme into matrix form, we obtain

$$(a_1^{k-1}, a_1^{k}, a_2^{k-1}, a_2^{k})^{T} = A_1(a_1^{k-2}, a_1^{k-1}, a_2^{k-2}, a_2^{k-1})^{T}, \tag{4.21}$$

where $A_1$is the Jacobian matrix (iteration matrix) given by

$$A_1 = \begin{bmatrix} 0 & 1 & 0 & 0 \\ e^{-\gamma\tau} & C_1\gamma\tau & 0 & 2C_1\tau \\ 0 & 0 & 0 & 1 \\ 0 & -2C_1\tau & e^{-\gamma\tau} & -C_1\gamma\tau \end{bmatrix}, \tag{4.22}$$

where $C_1 = 1/(\alpha e^{\gamma\tau} - \alpha + 1)$.

To analyze the stability of scheme (4.21), by straightforward calculations, we obtain the eigenvalues of A_1

$$\lambda_j = \pm\frac{1}{2}\left(4e^{-\gamma\tau} - 2C_1^2\tau^2(4-\gamma^2) \pm 2C_1\tau\left(C_1^2\tau^2(4-\gamma^2)^2 - 4e^{-\gamma\tau}(4-\gamma^2)\right)^{1/2}\right)^{1/2}$$

for $j = 1, \ldots, 4$. When $\gamma \in [0, 2]$,we have $\mod(\lambda_j) = e^{-\gamma\tau/2}$,the only chance that $\mod(\lambda_j) = 1$is the case when setting $\gamma = 0$,this can be seen from: $C_1 = 1$,the eigenvalues $\lambda_j$can be simplified to

$$\lambda_j = \pm(1 - 2\tau^2 \pm 2\tau\sqrt{\tau^2 - 1})^{1/2} \quad \text{for} \quad j = 1, \ldots, 4,$$

which is 1 in modulus and simple for $\tau \in [0, 1]$.

Case 2(P1M2O2): Set $\alpha = 1/2$for simplicity, substitute the Birkhoffian representation (4.20) into scheme **P1M2O2** (3.10) and write the result into matrix form, we obtain

$$(a_1^{k,-}, a_1^{k,+}, a_2^{k,-}, a_2^{k,+})^T = A_2(a_1^{k-1,-}, a_1^{k-1,+}, a_2^{k-1,-}, a_2^{k-1,+})^T, \tag{4.23}$$

where $A_2$is the Jacobian matrix given by

$$A_2 = C_2\begin{bmatrix} D_1D_5 & D_3 & 8\tau D_5 & 8\tau \\ D_3D_5^2 & D_1D_5 & 8\tau D_5^2 & 8\tau D_5 \\ -8\tau D_5 & -8\tau & D_2D_5 & D_4 \\ -8\tau D_5^2 & -8\tau D_5 & D_4D_5^2 & D_2D_5 \end{bmatrix}, \tag{4.24}$$

in which $C_2 = 1/(16 + 4\tau^2 - \gamma^2\tau^2)$, $D_1 = 16 + 4\gamma\tau$, $D_2 = 16 - 4\gamma\tau$, $D_3 = \gamma^2\tau^2 + 4\gamma\tau - 4\tau^2$, $D_4 = \gamma^2\tau^2 - 4\gamma\tau - 4\tau^2$, $D_5 = e^{-\frac{1}{2}\gamma\tau}$.

The eigenvalues $\lambda_j (j = 1, \ldots, 4)$of matrix $A_2$are

$$e^{-\frac{1}{2}\gamma\tau}(\text{degree } 2), \quad C_2e^{-\frac{1}{2}\gamma\tau}\left(16 - 4\tau^2 + \gamma^2\tau^2 \pm 8\tau i\sqrt{4-\gamma^2}\right).$$

Straightforward calculation gives $\mod(\lambda_j) = e^{-\gamma\tau/2} (j = 1, \ldots, 4)$,which is always less than 1 for $\gamma \in (0, 2], \tau > 0$, and exactly equal to 1 for $\gamma = 0$.

Case 3(P2S3O3): In this case, eigenvalues of the Jacobian matrix are too complex to present here. The linear stability can be verified by calculating the eigenvalues numerically. Actually, numerical tests for this scheme in Section 5 tell the same fact and attain the third-order of accuracy.

Remark 4.2. One main feature of the DGVIs is the discontinuous solutions at nodal points, or in other words, we have two values $a_j^{k,\pm}$near $t_k$for each a_j,which may cause repeated eigenvalues of the expanded iteration matrix A_2(4.24). When $\gamma = 0$,to see that the repeated eigenvalues does not violate the root condition [29, Theorem 3.3.14], we use the averages $\widetilde{a}_j^k = (a_j^{k,+} + a_j^{k,-})/2$for $j = 1, 2$and $k = 1, 2, \ldots, K$,then (4.23) can be simplified to

$$(\widetilde{a}_1^k,\ \widetilde{a}_2^k)^T = \frac{1}{4+\tau^2}\begin{bmatrix} 4-\tau^2 & 4\tau \\ -4\tau & 4-\tau^2 \end{bmatrix}(\widetilde{a}_1^{k-1},\ \widetilde{a}_2^{k-1})^T, \tag{4.25}$$

where the iteration matrix has two distinct eigenvalues

$$\lambda_{1,2} = \frac{4 - \tau^2 \pm 4\tau i}{4 + \tau^2}, \tag{4.26}$$

which is 1 in modulus.

4.3. Error estimates

In the above Section 4.2, we have showed the linear stability of the three DGVIs considering the example of linear damped oscillators (4.19). Now we turn to the order of accuracy for schemes **P0L1O1** (4.21), **P1M2O2** (4.23) and **P2S3O3** (3.11).

Theorem 4.2. *For linear damped oscillators (4.19), scheme **P0L1O1** (4.21) is of first-order accuracy, **P1M2O2** (4.23) is of second-order accuracy, and scheme **P2S3O3** applied to the case $\gamma = 0$is of third-order accuracy.*

Proof. (1) **(P0L1O1)**: First we rewrite scheme (4.21) as

$$\begin{cases} (1 - \alpha + \alpha e^{\gamma\tau})a_1^k - (\alpha + (1-\alpha)e^{-\gamma\tau})a_1^{k-2} - \tau(2a_2^{k-1} + \gamma a_1^{k-1}) = 0, \\ (1 - \alpha + \alpha e^{\gamma\tau})a_2^k - (\alpha + (1-\alpha)e^{-\gamma\tau})a_2^{k-2} + \tau(2a_1^{k-1} + \gamma a_2^{k-1}) = 0. \end{cases} \tag{4.27}$$

Noting the Taylor series expansions of $e^{\pm\gamma\tau}$and $a_j (j = 1, 2)$,we obtain

$$e^{\pm\gamma\tau} = 1 \pm \gamma\tau + O(\tau^2), \tag{4.28a}$$

$$a_j(t_k) = a_j(t_{k-1}) + \tau \dot{a}_j(t_{k-1}) + \frac{\tau^2}{2}\ddot{a}_j(t_{k-1}) + \frac{\tau^3}{6}\dddot{a}_j(t_{k-1}) + O(\tau^4), \quad \text{for} \quad j = 1, 2, \tag{4.28b}$$

$$a_j(t_{k-2}) = a_j(t_{k-1}) - \tau \dot{a}_j(t_{k-1}) + O(\tau^2), \quad \text{for } j = 1, 2. \tag{4.28c}$$

Replacing the coefficients and numerical solutions a_i^jin (4.27) by the related ones in (4.28), then collecting the common terms, we have

$$\begin{cases} a_1(t_k) - (1-\gamma\tau)a_1(t_{k-2}) - 2\tau a_2(t_{k-1}) - \gamma\tau a_1(t_{k-1}) = 2\tau(\dot{a}_1 - a_2)(t_{k-1}) + O(\tau^2), \\ a_2(t_k) - (1-\gamma\tau)a_2(t_{k-2}) + 2\tau a_1(t_{k-1}) + \gamma\tau a_2(t_{k-1}) = 2\tau(\dot{a}_2(t_{k-1}) + \gamma a_2(t_{k-1}) + a_1(t_{k-1})) + O(\tau^2), \end{cases} \tag{4.29}$$

which means (4.27) has a second-order local truncation error approximating system

$$\begin{cases} \dot{a}_1 - a_2 = 0, \\ \dot{a}_2 + \gamma a_2 + a_1 = 0, \end{cases} \tag{4.30}$$

that is, the linear damped oscillators (4.19).

(2) **(P1M2O2)**: For convenience, we give the nodal error of $a_1^k$by assuming $\alpha = 1/2$and

$$a_1(t_{k-1}) = a_1^{k-1,-} = a_1^{k-1,+}. \tag{4.31}$$

In this case, since discontinuous linear functions are used in approximating a_1,one may have two values near t_k,$a_1^{k,+}$and $a_1^{k,-}$. To consider the nodal error at point t_k,we use the average $\tilde{a}_j^k = (a_j^{k,+} + a_j^{k,-})/2$, for $j = 1, 2$as the numerical solution at t_k.

In the same manner as (1), by expanding the coefficients to the third power of τ,and regrouping the unknowns in **P1M2O2** (4.23), we have

$$\tilde{a}_1^k - \tilde{a}_1^{k-1} - \tau\tilde{a}_2^{k-1} + \frac{\tau^2}{16}\left((4+\gamma^2)a_1^{k-1,-} + (4-\gamma^2)a_1^{k-1,+}\right) + \frac{\gamma\tau^2}{8}\left(3a_2^{k-1,-} + a_2^{k-1,+}\right) = O(\tau^3). \tag{4.32}$$

Then, replacing the first term of (4.32) by exact solutions in equation (4.28 b) leads to

$$LTE = 2\tau(\dot{a}_1(t_{k-1}) - a_2(t_{k-1})) + \tau^2(\ddot{a}_1(t_{k-1}) + \gamma a_2(t_{k-1}) + a_1(t_{k-1})) = O(\tau^3), \tag{4.33}$$

in which LTEdenotes the local truncation error at t_k.

(3) **(P2S3O3)**: Again, we consider the nodal error of $a_1$and assume $\alpha = 1/2, \gamma = 0$to simplify the notation. Then for the linear damped oscillators (4.19), scheme (3.11) reduces to

$$(a_1^{k,-}, a_1^{k,+}, a_2^{k,-}, a_2^{k,+})^T = A_3(a_1^{k-1,-}, a_1^{k-1,+}, a_2^{k-1,-}, a_2^{k-1,+})^T, \tag{4.34}$$

where $A_3$is the Jacobian matrix

$$A_3 = C_3\begin{bmatrix} -3\tau^2 & 4D_6 & 12\tau & \tau D_6 \\ 4D_6 & -\frac{\tau^2}{3}D_7 & \tau D_6 & \frac{4\tau}{3}D_7 \\ -12\tau & -\tau D_6 & -3\tau^2 & 4D_6 \\ -\tau D_6 & -\frac{4\tau}{3}D_7 & 4D_6 & -\frac{\tau^2}{3}D_7 \end{bmatrix}, \tag{4.35}$$

in which $C_3 = 1/(16+\tau^2)$, $D_6 = 4-\tau^2$, $D_7 = 9-\tau^2$.

Regrouping the unknowns in (4.34) and using the Taylor expansion of the components of the Jacobian matrix A_3,we obtain

$$\tilde{a}_1^k - \tilde{a}_1^{k-1} - \tau\tilde{a}_2^{k-1} + \frac{\tau^2}{2}\tilde{a}_1^{k-1} + \tau^3\left(\frac{5}{48}a_2^{k-1,+} + \frac{3}{48}a_2^{k-1,-}\right) = O(\tau^4). \tag{4.36}$$

Then, in a similar way that leads to (4.29) and (4.33), we obtain the fourth-order local truncation error of **P2S3O3**.

Clearly, (4.29), (4.33) and (4.36) introduced local errors proportional to $\tau^2, \tau^3$and τ^4,respectively, which will exhibit $\tau, \tau^2$and $\tau^3$for the cumulative errors. □

5. Numerical examples

An important advantage of the symplecticity is the conservation of quadratic invariants for the discrete flow. On the other hand, excluding the quadratic case, incorporation of the energy-conserving method and symplecticity is extremely nontrivial [12]. In this section, for the linear damped oscillators (4.19) and Hojman–Urrutia Eq. (5.6), which have quadratic Birkhoffians, we verify the symplecticity of the three schemes **P0L1O1** (3.6), **P1M2O2** (3.10) and **P2S3O3** (3.11) using Definition 4.1. For each scheme, we also give the order of accuracy of numerical solution and the comparison of numerical Birkhoffians with exact ones.

To evaluate the error of the numerical solutions, we use L_{err}^{∞}norm (5.1) for scheme **P0L1O1**, L_{err}^{∞}norm (5.2) for schemes **P1M2O2** and **P2S3O3**, L_{err}^{2}norm (5.3) for all of the above three schemes. For simplicity, the error is given using $a_1^{\tau}$for linear

Table 1
The order of accuracy of scheme **P0L1O1** (4.21).

time step	L_{err}^{∞}	order	L_{err}^{2}	order
τ	3.0827e-01	-	1.0952e+00	-
$\tau/2$	9.6570e-02	1.6746	3.6610e-01	1.5809
$\tau/4$	3.5139e-02	1.4585	1.5253e-01	1.2631
$\tau/8$	1.4598e-02	1.2673	7.1963e-02	1.0838
$\tau/16$	6.6034e-03	1.1445	3.5423e-02	1.0225
$\tau/32$	3.1358e-03	1.0744	1.7641e-02	1.0057
$\tau/64$	1.5637e-03	1.0339	8.8118e-03	1.0014

Table 2
The order of accuracy of scheme **P1M2O2** (4.23).

time step	L_{err}^{∞}	order	L_{err}^{2}	order
τ	1.1159e-01	-	4.6406e-01	-
$\tau/2$	2.7961e-02	1.9967	1.1625e-01	1.9971
$\tau/4$	6.9923e-03	1.9996	2.9075e-02	1.9993
$\tau/8$	1.7483e-03	1.9998	7.2697e-03	1.9998
$\tau/16$	4.3708e-04	2.0000	1.8175e-03	1.9999
$\tau/32$	1.0927e-04	2.0000	4.5442e-04	1.9999
$\tau/64$	2.7318e-05	2.0000	1.1364e-04	1.9996

Table 3
The order of accuracy of scheme **P2S3O3** (5.5).

time step	L_{err}^{∞}	order	L_{err}^{2}	order
τ	3.4512e-05	-	1.6691e-04	-
$\tau/2$	2.5780e-06	3.7428	1.6575e-05	3.3320
$\tau/4$	2.3211ee-07	3.4734	1.9151e-06	3.1135
$\tau/8$	2.8877e-08	3.0068	2.3424e-07	3.0314
$\tau/16$	3.6018e-09	3.0031	2.9116e-08	3.0081
$\tau/32$	4.4984e-10	3.0013	3.6346e-09	3.0019
$\tau/64$	5.6255e-11	2.9993	4.5852e-10	2.9868

damped oscillators and a_2^{τ} for the Hojman–Urrutia equations, respectively, other variables a_i^{τ} also maintain the corresponding order of different schemes.

$$L_{err}^{\infty} = \max_{1\le k\le K} \left| a_i^k - a_i(t_k) \right|, \tag{5.1}$$

$$\text{or} \quad L_{err}^{\infty} = \max_{1\le k\le K} \left| a_i^{k-\frac{1}{2}} - a_i(t_{k-\frac{1}{2}}) \right|, \tag{5.2}$$

$$L_{err}^{2} = \sqrt{\sum_{k=1}^{K} \int_{t_{k-1}}^{t_k} \left(a_i^{\tau} - a_i(t) \right)^2 \mathrm{d}t}. \tag{5.3}$$

5.1. Linear damped oscillator

Case 1(P0L1O1): To show the symplecticity of scheme **P0L1O1** for linear damped oscillator (4.21), recall the Jacobian matrix A_1(4.22) and the structure matrix $G(t_k, \boldsymbol{a}^k)$given by

$$G(t_k, \boldsymbol{a}^k) = \begin{bmatrix} 0 & 0 & 0 & -e^{\gamma t_k} \\ 0 & 0 & -e^{\gamma t_k} & 0 \\ 0 & e^{\gamma t_k} & 0 & 0 \\ e^{\gamma t_k} & 0 & 0 & 0 \end{bmatrix}. \tag{5.4}$$

A straightforward calculation verifies the equality (4.2), that is, $A_1^T G(t_k, \boldsymbol{a}^k) A_1 = G(t_{k-1}, \boldsymbol{a}^{k-1})$.

Using $\alpha = 0.5, \tau = 0.1$and refined step sizes, Table 1, 2 and 3 give the order of accuracy in $L_{err}^{\infty}$and L_{err}^{2}norms, respectively, of the numerical solutions computed through different DGVIs.

Case 2(P1M2O2): Similar to **Case 1**, symplecticity of (4.23) can be verified by $A_2^T G(t_k, \boldsymbol{a}^k) A_2 = G(t_{k-1}, \boldsymbol{a}^{k-1})$,where $A_2$is given in (4.24).

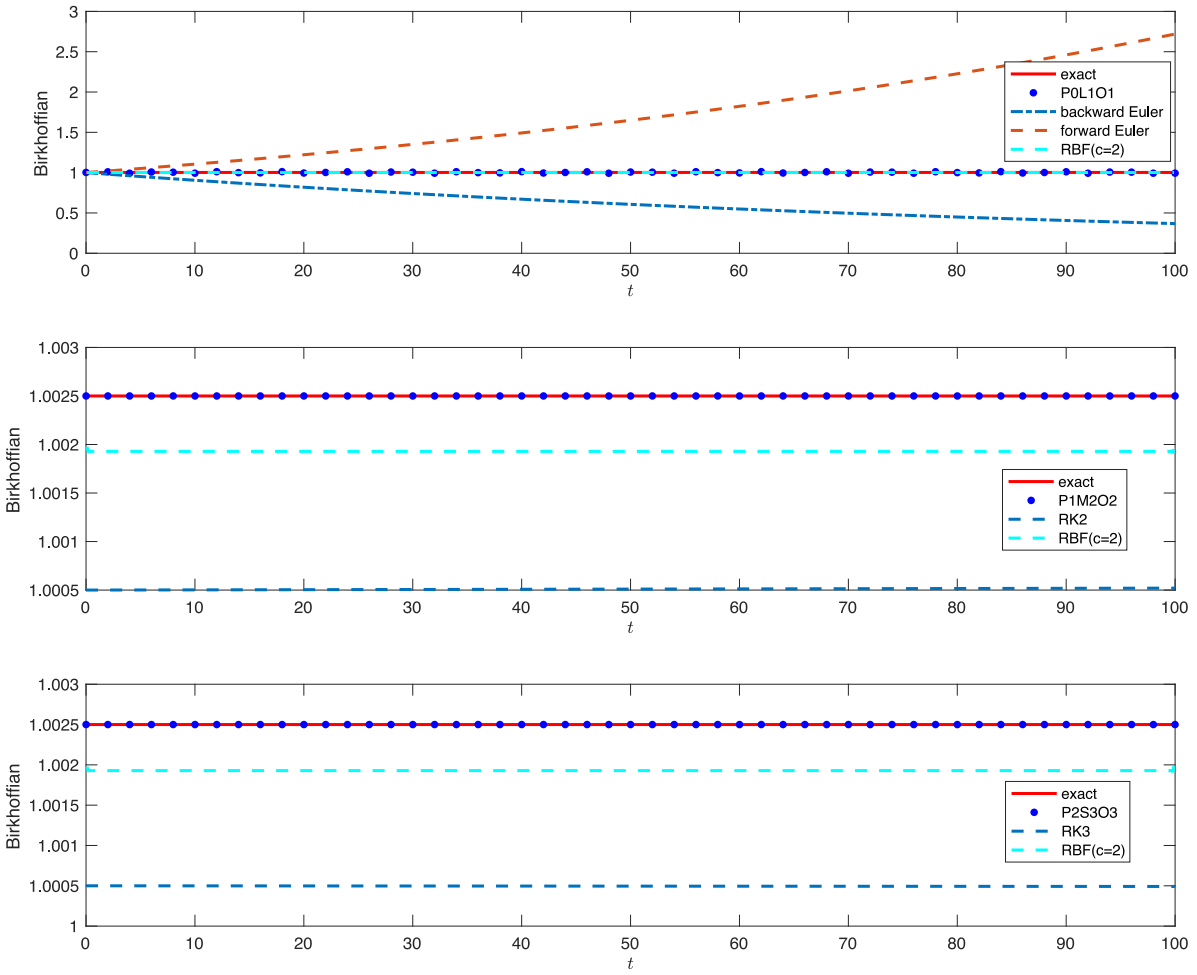

Fig. 1. Comparison of Birkhoffians computed through DGVIs, classical Runge–Kutta methods and RBF methods for linear damped oscillator (4.19).

Case 3(P2S2O3): For linear damped oscillator (4.19), **P2S2O3** reads

$$\begin{cases} 4(1+e^{\frac{1}{2}\gamma\tau})a_2^{k-\frac{1}{2}} - (1+e^{\gamma\tau})a_2^{k,-} - 6a_2^{k-1,-} + \tau(2a_1^{k-1,+} + \gamma a_2^{k-1,+}) = 0, \\ \quad (e^{\frac{1}{2}\gamma\tau} + e^{\gamma\tau})a_2^{k,-} - (1+e^{\frac{1}{2}\gamma\tau})a_2^{k-1,+} + \tau e^{\frac{1}{2}\gamma\tau}(2a_1^{k-\frac{1}{2}} + \gamma a_2^{k-\frac{1}{2}}) = 0, \\ (1+e^{\gamma\tau})a_2^{k-1,+} - 4(e^{\gamma\tau} + e^{\frac{1}{2}\gamma\tau})a_2^{k-\frac{1}{2}} + 6e^{\gamma\tau}a_2^{k,+} + \tau e^{\gamma\tau}(2a_1^{k,-} + \gamma a_2^{k,-}) = 0, \\ 4(1+e^{\frac{1}{2}\gamma\tau})a_1^{k-\frac{1}{2}} - (1+e^{\gamma\tau})a_1^{k,-} - 6a_1^{k-1,-} - \tau(2a_2^{k-1,+} + \gamma a_1^{k-1,+}) = 0, \\ (e^{\frac{1}{2}\gamma\tau} + e^{\gamma\tau})a_1^{k,-} - (1+e^{\frac{1}{2}\gamma\tau})a_1^{k-1,+} - \tau e^{\frac{1}{2}\gamma\tau}(2a_2^{k-\frac{1}{2}} + \gamma a_1^{k-\frac{1}{2}}) = 0, \\ \quad (1+e^{\gamma\tau})a_1^{k-1,+} - 4(e^{\gamma\tau} + e^{\frac{1}{2}\gamma\tau})a_1^{k-\frac{1}{2}} + 6e^{\gamma\tau}a_1^{k,+} - \tau e^{\gamma\tau}(2a_2^{k,-} + \gamma a_1^{k,-}) = 0. \end{cases} \tag{5.5}$$

In **Case 3**, the symplecticity of scheme **P2S3O3** (5.5) can be verified through symbolic manipulation in MATLAB. In Figs. 1and 2, for all the three DGVIs, we use the following parameters.

Method parameters: $\alpha = 0.5, \gamma = 0.001, \tau = 0.01.$

Initial conditions $\begin{cases} \textbf{P0L1O1 (4.21)}: a_1^{-1} = a_1^0 = a_2^{-1} = a_2^0 = 1, \\ \textbf{P1M2O2} \text{ (4.23)}, \textbf{P2S3O3} \text{ (5.5)}: a_1^{0,+} = a_1^{0,-} = a_2^{0,+} = a_2^{0,-} = 1. \end{cases}$

For the RBF method, we choose the shape parameter $c = 2$.

As a result, the numerical Birkhoffians computed through the DGVIs are much better than that through the Runge–Kutta type schemes and RBF methods, in matching the exact Birkhoffians. It seems that the first-order Kong's method (P0R1O1) is outperforming P0L1O1 in preserving the Birkhoffians, however, supplementary comparisons in Birkhoffian errors given in Fig. 2 for the second order (P1M2O2) and the third order (P2S3O3) schemes, show that the DGVIs remain valid in improving both the order of accuracy and the accuracy of preserving Birkhoffians against the method derived in [16].

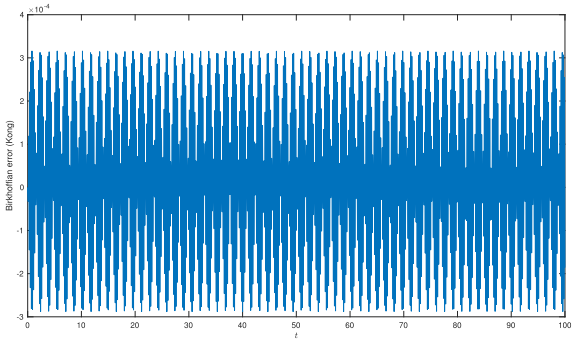

(a) The first-order Kong's method (P0R1O1) in [16]

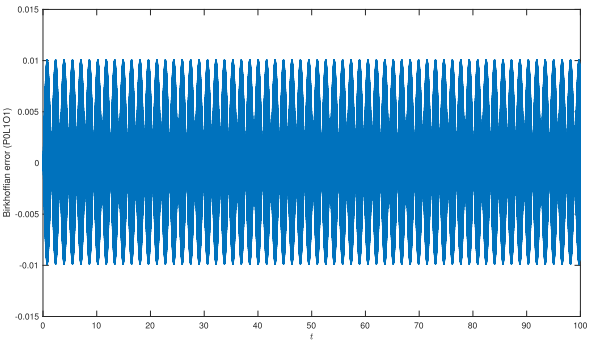

(b) P0L1O1

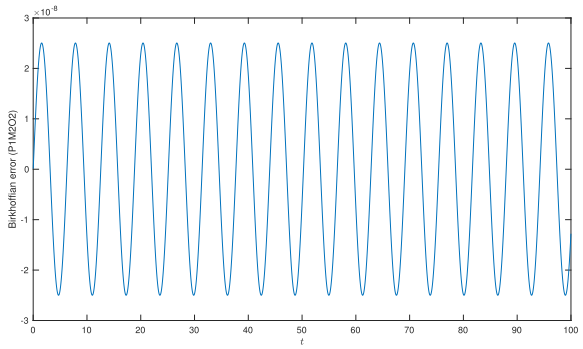

(c) P1M2O2

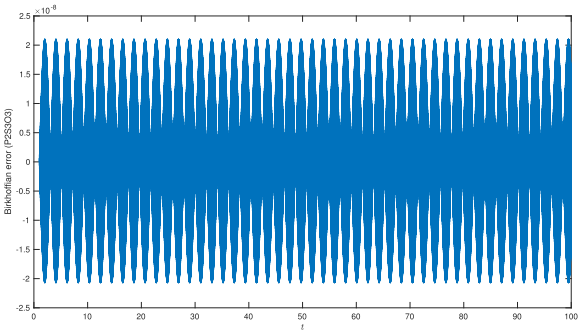

(d) P2S3O3

Fig. 2. Comparison of Birkhoffian errors computed through DGVIs and methods used in [16] for (4.19).

Table 4
The order of accuracy of scheme **P0L1O1** (3.6).

time step	L^{∞}_{err}	order	L^{2}_{err}	order
τ	1.8315e-01	-	1.1254e+00	-
$\tau/2$	5.1229e-02	1.8380	3.7576e-01	1.5825
$\tau/4$	2.5310e-02	1.0173	1.5628e-01	1.2657
$\tau/8$	1.2578e-02	1.0088	7.3672e-02	1.0849
$\tau/16$	6.2695e-03	1.0045	3.6256e-02	1.0229
$\tau/32$	3.1299e-03	1.0022	1.8055e-02	1.0058
$\tau/64$	1.5637e-03	1.0011	9.0184e-03	1.0015

5.2. Hojman–Urrutia equations

In [3], Hojman and Urrutia give the following equations

$$\ddot{x}+\dot{y}=0,\ \ \ddot{y}+y=0, \tag{5.6}$$

which do not have a Hamiltonian representation, but have a Birkhoffian representation if setting $a_1=x, a_2=y, a_3=\dot{x}, a_4=\dot{y}$and

$$\begin{cases} R_1(t,\mathbf{a}) &= a_2+a_3,\ R_2(t,\mathbf{a})=0,\ R_3(t,\mathbf{a})=a_4,\ R_4(t,\mathbf{a})=0,\\ B(t,\mathbf{a}) &= \frac{1}{2}\big[(a_3)^2+2a_2a_3-(a_4)^2\big], \end{cases}$$

in the Birkhoffian system (1.1).

Setting $\alpha=0.5, \tau=0.1$and refined step sizes, Table 4, 5 and 6 list the order of accuracy of the numerical solution computed through different DGVIs.

Table 5
The order of accuracy of scheme **P1M2O2** (3.10).

time step	L_{err}^{∞}	order	L_{err}^{2}	order
τ	1.1550e-01	-	4.7875e-01	-
$\tau/2$	2.8918e-02	1.9979	1.1983e-01	1.9983
$\tau/4$	7.2325e-03	1.9994	2.9965e-02	1.9996
$\tau/8$	1.8083e-03	1.9998	7.4918e-03	1.9999
$\tau/16$	4.5210e-04	2.0000	1.8730e-03	2.0000
$\tau/32$	1.1302e-04	2.0000	4.6824e-04	2.0000
$\tau/64$	2.8256e-05	2.0000	1.1706e-04	2.0000

Table 6
The order of accuracy of scheme **P2S3O3** (3.11).

time step	L_{err}^{∞}	order	L_{err}^{2}	order
τ	4.2912e-05	-	1.7151e-04	-
$\tau/2$	3.5536e-06	3.5940	1.7005e-05	3.3342
$\tau/4$	3.3307e-07	3.4154	1.9634e-06	3.1146
$\tau/8$	3.4881e-08	3.2553	2.4009e-07	3.0317
$\tau/16$	3.9587e-09	3.1394	2.9843e-08	3.0082
$\tau/32$	4.7221e-10	3.0675	3.7252e-09	3.0020
$\tau/64$	5.9228e-11	2.9951	4.6990e-10	2.9869

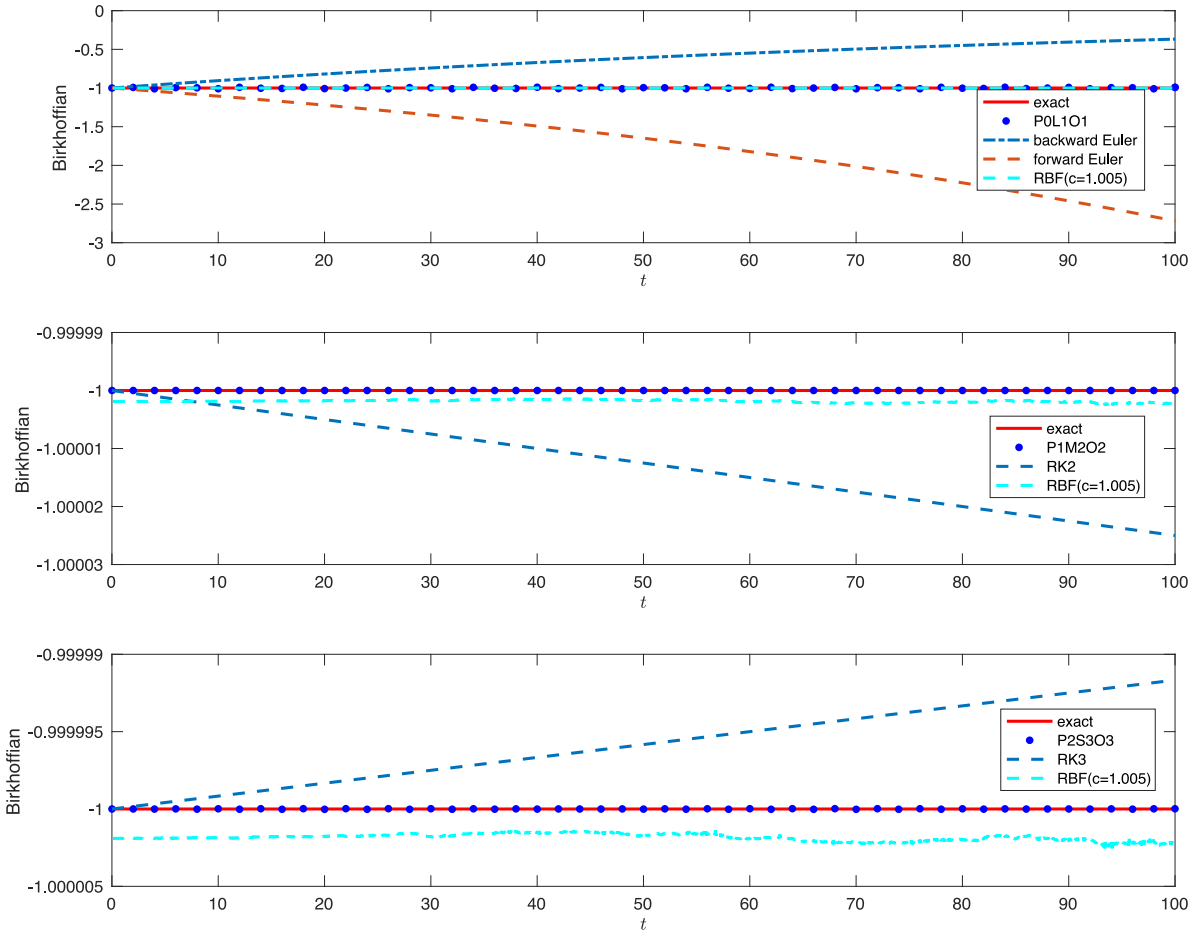

Fig. 3. Comparison of Birkhoffians computed through DGVIs, classical Runge–Kutta methods and RBF methods for Hojman–Urrutia Eq. (5.6).

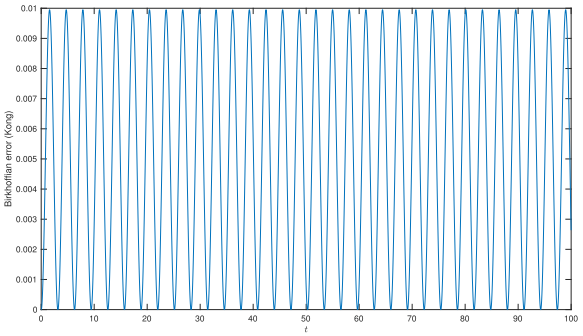

(a) The first-order Kong's method (P0R1O1) in [16]

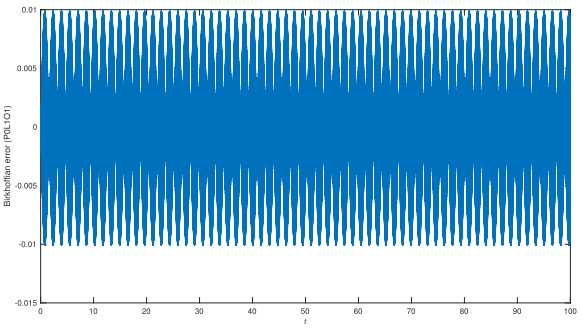

(b) P0L1O1

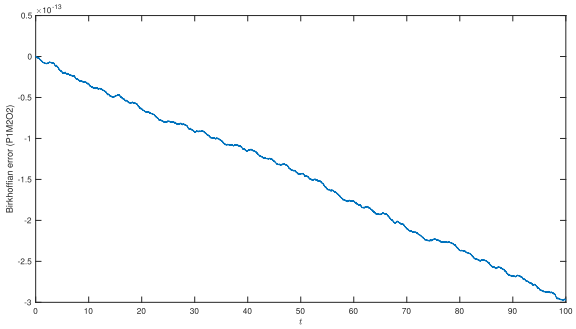

(c) P1M2O2

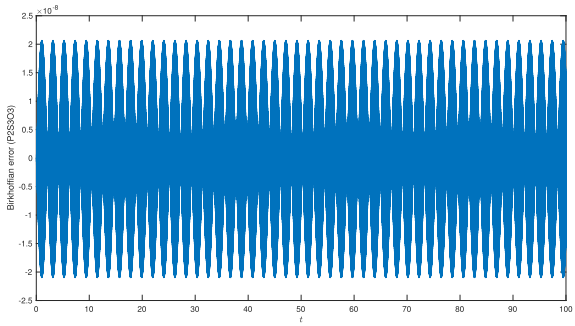

(d) P2S3O3

Fig. 4. Comparison of Birkhoffian errors computed through DGVIs and methods used in [16] for (5.6).

In Figs. 3 and 4, for all the three DGVIs, we use the following parameters.

$$\text{Method parameters:}\quad \alpha = 0.5,\ \tau = 0.01.$$

$$\text{Initial conditions}\begin{cases} \textbf{P0L1O1 (4.21)}: a_1^{-1} = a_1^0 = 2, & a_2^{-1} = a_2^0 = -1, \quad a_3^{-1} = a_3^0 = a_4^{-1} = a_4^0 = 1, \\ \textbf{P1M2O2}\ (4.23),\ \textbf{P2S3O3}\ (5.5): & a_1^{0,+} = a_1^{0,-} = 2, \quad a_2^{0,+} = a_2^{0,-} = -1, \\ & a_3^{0,+} = a_3^{0,-} = a_4^{0,+} = a_4^{0,-} = 1. \end{cases}$$

For the RBF method, we choose the shape parameter $c = 1.005$.

We would like to comment that, it seems that Fig. 4(c) shows a decreasing function for the Birkhoffian error, but considering the scale (vertical axis) of the figure, the **P1M2O2** scheme provides the most accurate Birkhoffian among the four methods.

6. Concluding remarks

We constructed three novel discontinuous Galerkin variational integrators (**P0L1O1, P1M2O2** and **P2S3O3**) for Birkhoffian system (1.1). These integrators are based on the discontinuous Galerkin time discretization techniques combined with numerical quadrature of the Birkhoffian variational formulation. The first- and second- order schemes in [16] are shown to be special cases of the first- and second-order DGVIs (Remark 3.1). Moreover, for the three schemes mentioned above, we prove the symplecticity rigorously and illustrate the linear stability and order of accuracy considering the example of linear damped oscillators. Finally, we test these schemes with linear damped oscillators and Hojman–Urrutia equations, where the later cannot be written into Hamiltonian system. Numerical results verify the stability, preservation of the quadratic Birkhoffians and the order of accuracy of these schemes.

Declaration of Competing Interest

We declare that we have no conflict of interest.

Acknowledgments

The authors would like to thank the anonymous referees for valuable suggestions which led to significant improvements in this revised version. This work was supported by the National Natural Science Foundation of China under Grant No. 11672032.

References

[1] R.M. Santilli, Foundations of Theoretical Mechanics II, Springer, New York, 1982.
[2] F. Mei, R. Shi, Y. Zhang, H. Wu, Dynamics of Birkhoff systems (in Chinese), Beijing Insti. Tech. Press, 1996.
[3] S. Hojman, L.F. Urrutia, On the inverse problem of the calculus of variations, J. Math. Phys. 22 (9) (1981) 1896–1903.
[4] F. Riewe, Mechanics with fractional derivatives, Phys. Rev. E 55 (3) (1997) 3581–3592.
[5] J. Stoer, R. Bulirsch, Introduction to Numerical Analysis, 12, Springer, New York, 2013.
[6] H. Zheng, Z. Yang, C. Zhang, M. Tyrer, A local radial basis function collocation method for band structure computation of phononic crystals with scatterers of arbitrary geometry, Appl. Math. Model. 60 (2018) 447–459.
[7] M.C. Delfour, W. Hager, F. Trochu, Discontinuous Galerkin methods for ordinary differential equations, Math. Comp. 36 (154) (1981) 455–473.
[8] M.C. Delfour, F. Dubeau, Discontinuous polynomial approximations in the theory of one-step, hybrid and multistep methods for nonlinear ordinary differential equations, Math. Comp. 47 (175) (1986) 169–189.
[9] S. Zhao, G.W. Wei, A unified discontinuous Galerkin framework for time integration, Math. Methods Appl. Sci. 37 (7) (2014) 1042–1071.
[10] L. Brugnano, G. Gurioli, F. Iavernaro, Analysis of energy and quadratic invariant preserving (equip) methods, J. Comput. Appl. Math. 335 (2018) 51–73.
[11] L. Brugnano, F. Iavernaro, D. Trigiante, Energy and quadratic invariants preserving integrators of gaussian type, AIP Conf. Proc. 1281 (2010) 227–230.
[12] L. Brugnano, F. Iavernaro, D. Trigiante, Energy and quadratic invariants preserving integrators based upon gauss collocation formulae, SIAM J. Numer. Anal. 50(6) (2012) 2897–2916.
[13] L. Brugnano, G. Gurioli, F. Iavernaro, Predictor-corrector implementation of equip methods, AIP Conf. Proc. 1978 (1) (2018) 120004.
[14] J.M. Wendlandt, J.E. Marsden, Mechanical integrators derived from a discrete variational principle, Phys. D. 106 (3–4) (1997) 223–246.
[15] M. Leok, J. Zhang, Discrete Hamiltonian variational integrators, IMA J. Numer. Anal. 31 (4) (2011) 1497–1532.
[16] X.L. Kong, H.B. Wu, F.X. Mei, Structure-preserving algorithms for Birkhoffian systems, J. Geom. Phys. 62 (5) (2012) 1157–1166.
[17] X.L. Kong, H.B. Wu, F.X. Mei, Variational integrators for forced Birkhoffian systems, Appl. Math. Comput. 225 (2013) 326–332.
[18] J. Cortes, S. Martinez, Non-holonomic integrators, Nonlinearity 14 (5) (2001). 1365–1392(28)
[19] R.C. Fetecau, J.E. Marsden, M. Ortiz, M. West, Nonsmooth lagrangian mechanics and variational collision integrators, SIAM J. Appl. Dyn. Syst. 2 (3) (2003) 381–416.
[20] O. Junge, J.E. Marsden, S. Ober-Blöbaum, Discrete mechanics and optimal control, IFAC Proc. Vol. 38 (1) (2005) 538–543.
[21] S. Leyendecker, S. Ober-Blöbaum, J.E. Marsden, M. Ortiz, Discrete mechanics and optimal control for constrained systems, Optimal Control Appl. Methods. 31 (6) (2009) 505–528.
[22] J.E. Marsden, M. West, Discrete mechanics and variational integrators, Acta Math. 10 (2001) 357–514.
[23] E. Gagarina, V.R. Ambati, J.J.W. van der Vegt, O. Bokhove, Variational space-time (dis)continuous Galerkin method for nonlinear free surface water waves, J. Comput. Phys. 275 (2014) 459–483.
[24] E. Gagarina, V.R. Ambati, S. Nurijanyan, J.J.W. van der Vegt, O. Bokhove, On variational and symplectic time integrators for Hamiltonian systems, J. Comput. Phys. 306 (2016) 370–389.
[25] J. Hall, M. Leok, Lie group spectral variational integrators, Found. Comput. Math. 17 (1) (2017) 199–257.
[26] E. Hairer, C. Lubich, G. Wanner, Geometric Numerical Integration: Structure-preserving Algorithms for Ordinary Differential Equations, 31, Springer, Berlin, 2006.
[27] H.L. Su, Y.J. Sun, M.Z. Qin, R. Scherer, Structure preserving schemes for Birkhoffian systems, Int. J. Pure Appl. Math. Sci. 40 (3) (2007) 341–366.
[28] J.E. Marsden, T.S. Ratiu, Introduction to Mechanics and Symmetry: A Basic Exposition of Classical Mechanical Systems, 17, Springer Science & Business Media, 2013.
[29] G. Dahlquist, A. Björck, Numerical Methods in Scientific Computing, I, SIAM, Philadelphia, 2008.